

## Acousto-optic and Electro-optic Modulators for Photonic Aharonov–Bohm Effect

光子アハラノフ・ボーム効果の発生に向けた  
音響光学・電気光学変調器

Yuya Hiramatsu<sup>‡</sup>, Masashi Suzuki, and Shoji Kakio (University of Yamanashi)  
平松裕也<sup>‡</sup>, 鈴木雅視, 垣尾省司 (山梨大学)

### 1. Introduction

Recently, attention has been focused on basic research on the photonic Aharonov–Bohm (AB) effect. The photonic AB effect is a phenomenon in which a light beam is affected by the gauge potential, and a nonreciprocal phase can be obtained. Li *et al.* showed that a nonreciprocal phase can be induced by using two bulk acousto-optic modulators (AOMs) in a tandem manner and that the photonic AB effect can be demonstrated by the interference between AOM and reference beams.<sup>1)</sup>

Here, we propose the use of two optical waveguide-type devices to produce the photonic AB effect. One is an AOM driven by two surface acoustic waves (SAWs), hereafter called the tandem AOM, as part of introducing a nonreciprocal phase delay through double diffraction. The other is an electro-optic modulator (EOM) used to produce the reference phase beam. The final aim of our experiments is to acquire the photonic AB effect caused by the optical waveguide device that monolithically integrates the AOM and EOM on the same substrate. Therefore, we should select a substrate with sufficient AO and EO characteristics to produce the photonic AB effect simultaneously.

In this study, a tandem AOM and an EOM using the annealed/proton-exchanged (APE) optical waveguide on a 128°-rotated Y-cut LiNbO<sub>3</sub> substrate (128°Y-cut LN) were investigated at an optical wavelength of 633 nm. In this paper, first, the configuration and fabrication of the tandem AOM and EOM are described. Then, the double diffraction properties of the tandem AOM are reported. Finally, the electro-optic constant evaluated by phase modulation is presented.<sup>2)</sup>

### 2. Configuration and Fabrication

#### 2.1. Tandem AOM

The overall configuration of the tandem AOM is shown in **Fig. 1**. The waveguide pattern was designed to interchange input and output (doubly diffracted) ports on the basis of the results of beam propagation analysis (OptiBPM 6.0 of

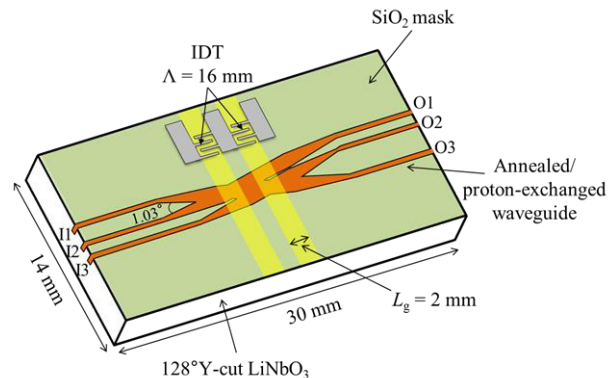


Fig. 1 Configuration of the tandem AOM.

Optiwave).<sup>3)</sup> The input light from port I2 is doubly diffracted by the first and second SAW propagations launched from interdigital transducers (IDTs) and then guided to port O2.

The channel waveguide was fabricated by first forming an RF-sputtered SiO<sub>2</sub> mask with a film thickness of 0.25 μm by the liftoff method on 128°Y-cut LN, and then carrying out the PE process and annealing. The PE time was 40 min in a solution of benzoic acid containing 0.2 mol% lithium benzoate at 240 °C, and the annealing time was 40 min at 400 °C. A Gaussian index profile with a change in  $\Delta n_e$  of 0.008 and a waveguide depth of 3.3 μm at  $\Delta n_e/e$  was obtained. After polishing the end face of the waveguide, IDTs with a period length  $\Lambda$  of 16 μm, 20 finger pairs and an overlap length of 2 mm were formed in the first and second SAWs.

#### 2.2. EOM

A conventional EO phase modulator consisting of a straight channel waveguide with strip electrodes was fabricated on 128°Y-cut LN. The PE time and annealing time were 1 h 15 min and 1 h 40 min, respectively, and  $\Delta n_e$  of 0.01 and a waveguide depth of 6.4 μm were obtained. After polishing the end face, SiO<sub>2</sub> thin film with a thickness of 0.25 μm was formed as a buffer layer, and two parallel strip electrodes with a gap of 10 μm and a length of 15 mm were formed using an aluminum film on the channel waveguide.

### 3. Experimental Results for Tandem AOM

First, the optical field distribution and diffraction property were simulated by BPM analysis. The maximum doubly diffracted power in port O2 was 0.45 when the input power to port I2 was 1.0. Then, diffraction properties were measured using a 633 nm laser at a driving frequency of approximately 250 MHz. To prevent the generation of heat due to the SAW power, a pulse-modulated RF voltage with a pulse width of 2 ms was supplied to the input IDTs.

**Figure 2** shows the measured diffraction properties at the input voltage supplied to the second SAW at the maximum diffraction efficiency by the first SAW. The solid lines in these figures indicate the fitted  $\sin^2$  curves. A peak diffraction efficiency of 29% was obtained by driving both SAWs at the same frequency. The leaked beam power of 13.4 dB was measured at port O2. When the input light was guided to port O2, similar diffraction properties were obtained. These properties are considered sufficient for observing the photonic AB effect with a nonreciprocal phase.

### 4. Evaluation of Electro-optic Constant

The bulk value of the electro-optic constant  $r_{33}^S$  on  $128^\circ\text{Y}$ -cut LN was calculated to be 33.6 pm/V by rotating the cut angle from the Z-cut; this value was higher than that of the Z-cut one. In addition, it is known that the electro-optic constant of the APE waveguide is approximately 70% of the bulk value.<sup>4)</sup> Thus,  $r_{33}^S$  was estimated to be 23.5 pm/V for the fabricated EOM.

The electro-optic constant was measured by phase modulation.<sup>2)</sup> The applied RF electric field is vertical to the substrate plane and perpendicular to the optical electric field of the TM mode. Therefore, the electro-optic constant sensed by the guided wave in the APE waveguide is  $r_{33}^S$ . An RF voltage at a frequency of 100 MHz was applied between the electrodes. The spectrum of the modulated output beam passing through a scanning Fabry–Perot interferometer was detected using a photomultiplier and observed on an oscilloscope. As a voltage  $V_{p-p}$  is applied, the power is shifted from the carrier to the sideband according to the degree of modulation.

The plots in **Fig. 3** show the phase modulation characteristic as a function of the applied voltage. The vertical axis is the ratio of the measured power in the carrier to that in the first sideband. The power ratio is given as the square of the ratio of the Bessel functions of the zeroth and first orders. The solid line shows the theoretical curve when  $r_{33}^S$  is 23.5 pm/V. It is revealed that the experimental value is generally consistent with the theoretical curve. Thus, the evaluated value of 23.5 pm/V was confirmed experimentally and

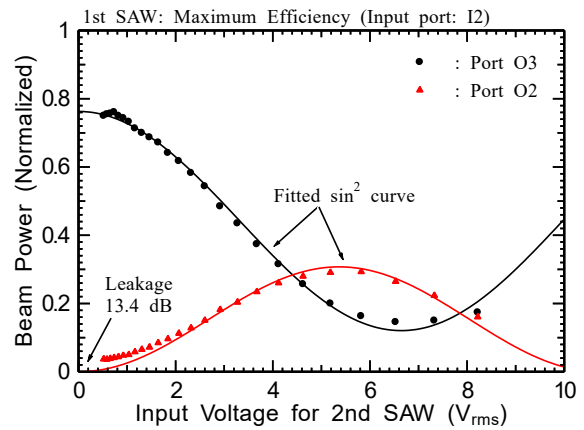


Fig. 2 Diffraction properties of tandem AOM.

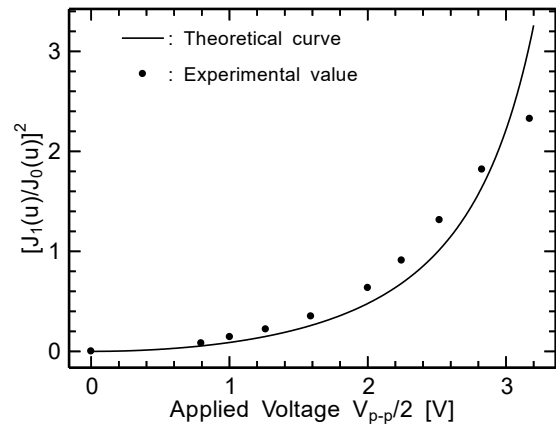


Fig. 3 Measured phase modulation characteristic.

corresponds to half-wave voltage of 5.5 V at a wavelength of 633 nm. It is also sufficient for observing the photonic AB effect.

### 5. Conclusions

To demonstrate the photonic AB effect, the AO and EO characteristics of APE waveguides fabricated on  $128^\circ\text{Y}$ -cut LN were investigated. First, the tandem AOM with interchangeable input and output ports was fabricated and a double-diffraction efficiency of 29% was measured. Then, the EOM was also fabricated and the electro-optic constant was measured. It was found that  $r_{33}^S$  (23.5 pm/V) in this case is higher than that of the Z-cut one. In the future, the photonic AB effect will be demonstrated using the waveguide-type AOM and EOM.

### References

1. E. Li, *et al.*: Nat. Commun. **5** (2014) 3225.
2. M. Minakata, *et al.*: Appl. Phys. Lett. **49** (1986) 992.
3. S. Kakio, S. Shinkai and Y. Nakagawa: Jpn. J. Appl. Phys. **49** (2010) 07HD18.
4. S. Kakio and M. Minakata: J. IEICE **J76-C-I** (1993) 514.